Effects of Di(2,2,2-trifluoroethyl) Carbonate on the Ignition Delay Time and Laminar Flame Speed of H_2 and CH_4

M. A. Turner[1], D. J. Mohr[1], P. Diévart[2], L. Catoire[2], E. L. Petersen[1], and O. Mathieu[1]

[1]J. Mike Walker '66 Department of Mechanical Engineering, Texas A&M University College Station, Texas, USA/[2]Unité de Chimie et des Procédés (UCP), ENSTA Paris, Institut Polytechnique de Paris, 91120 Palaiseau, France

1   Introduction

The market share of battery electric vehicles (BEV) is predicted to increase significantly within the next few years in most developed countries. This market share is already significant in Europe, where BEV outsold diesel-powered passenger cars in August, 2021. This upcoming large number of BEV on the road will be statistically accompanied by an increase of collisions involving these vehicles, possibly leading to a physical abuse of the Lithium-ion battery (LIB) by crushing or puncture. As described in Wang et al. [1], a physical abuse of a LIB can lead to an electric abuse, followed by a thermal abuse and potentially a fire that is very difficult to extinguish by means commonly used by first responders (*i.e.* water). Note that a similar fire hazard from LIB is possible in case of defect in the conception or manufacturing process of the battery, as seen in recent years with phones and cars.

To mitigate this fire hazard, the addition of specific fire suppressants to the battery electrolyte (the flammable liquid that allows lithium salt ions to move from one electrode to the other) is considered [2, 3]. Among those fire suppressants, di(2,2,2-trifluoroethyl) carbonate (DtFEC) is attractive [2] as it presents the same chemical structure as diethyl carbonate (DEC), a very common electrolyte component [4]. The similarity in the structure between these two components (see Fig. 1) makes DtFEC appealing as it is potentially less likely to degrade the battery performance through undesired physical and/or chemical processes.
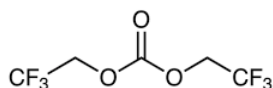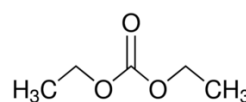
Di(2,2,2-trifluoroethyl) Carbonate (DtFEC)   Diethyl Carbonate (DEC)

Figure 1: Chemical structure of di(2,2,2-trifluoroethyl) carbonate (DtFEC) and diethyl carbonate (DEC).

To assess the fire suppressant properties of DtFEC, a method used in former studies from our group with various fire suppressants was utilized [5-7]. This method consists of using fuels for which the

combustion properties are well-known (H_2 and CH_4 here) as baselines, and to seed this mixture with a small amount of the fire suppressant. The observed change in the combustion properties allow probing the effectiveness of the fire suppressant. Here, neat mixtures of H_2 [8] and CH_4 [5, 9] were seeded with DtFEC at a concentration corresponding to 10% of the fuel concentration for the shock-tube measurements, and to 0.5% of the total mixture for the closed-vessel experiments. Experiments were conducted near atmospheric pressure for several equivalence ratios (ϕ), and results of this addition of DtFEC on the ignition delay time and laminar flame speed of H_2 and CH_4 are presented below.

2   Experimental methods

2.1   Shock tube and ignition delay time measurements

A stainless-steel shock tube (15.24-cm i.d., 4.72-m long and 7.62-cm i.d., 2.46-m long for the driven and driver sections, respectively) heated to 373 K was used to conduct the ignition delay time measurements. The shock tube was in a single-diaphragm configuration, and two polycarbonate diaphragms (0.25- and 0.13-mm thickness) were used for each experiment. The mixing tank and manifold were also heated to 373 K. The velocity of the incident shock wave was measured using five PCB-113B22 piezoelectric pressure transducers and extrapolated to the endwall to determine post reflected-shock conditions. A temperature uncertainty behind reflected shock waves (T_5) below 10 K was estimated. Test pressure was monitored on the sidewall (16 mm from the endwall, Kistler 603-B1) and on the endwall (PCB-113B22). Chemiluminescence from OH* and CH* were recorded at the sidewall location using an interference filter at 307 ± 10 nm for OH* and at 430 ± 15 nm for CH*. The test section was evacuated to 2×10^{-5} Torr or better using a roughing pump and a turbomolecular pump before each experiment. The ignition delay times presented herein were determined using the peak location of the OH* signal, with the reflected shock wave arrival at the sidewall location as time zero. The uncertainty for these measurements is estimated to be about 10%. Test mixtures were prepared manometrically in a stainless-steel mixing tank using O_2, Ar, H_2 (Praxair, 99.99%) and CH_4 (Praxair, 99.97%). DtFEC (TCI America, >98%) was introduced into the tank via a heated vial. The vial was degassed at least 3 times prior to introducing the fire suppressant into the mixing tank.

2.2   Closed vessel and laminar flame speed measurements

Spherically expanding flame experiments were conducted at room temperature (294.5 ± 0.5 K) using a 34-L cylindrical chamber. Gas mixtures were prepared manometrically in the chamber for each experiment, using the same H_2, CH_4, and DtFEC as described in Section 2.1 and synthetic air (Praxair; 21.0% O_2, 99.990%; 79.0% N_2, 99.998%). The rig's stirring fans homogenized the mixtures before ignition. Optical access for the schlieren diagnostic was provided by 12.7-cm diameter windows. An image analysis software relying on contrast adjustment and Canny edge detection was developed in-house to extract flame radii from the schlieren images. The rate of change of the flame radius is determined from the time history of the flame radius. The propagation speed of the flame relative to the burned gas was extrapolated to its unstretched value using nonlinear relationships between the burned flame speed and the stretch rate of the flame described in detail by Chen [10]. To arrive at the unstretched, unburned flame speed, continuity is applied, whereby the burned-gas speed is multiplied by the ratio of the densities of the burned and unburned gases. More detail on this analysis process is given by Sikes et al. [11]. The mixture densities were calculated using the equilibrium chemistry routine in Chemkin-Pro and the thermodynamic properties derived according to Section 3 below. The constant-pressure assumption was verified by recording time-synchronized chamber pressure during each experiment. Pressure rise was less than 1% during recorded flame propagation.

3   DtFEC Thermochemistry Calculation

The heat of formation of DtFEC was obtained through an atomization scheme. The most stable molecular structure and related vibrational frequencies were obtained in Gaussian 09 with the density functional [12] M06-2x-D3 (Grimme's dispersion correction [13] inclusive) in association with the Dunning augmented double-ζ basis set aug-cc-pVDZ. A series of single point energies calculations were then performed with Orca at the DLPNO-CCSD(T) and CCSD(T) methods with basis sets of increasing size (cc-pVDZ, cc-pVTZ, and cc-pVQZ) and extrapolated to the infinite basis set limit through a mixed exponential/Gaussian scheme. Ideal-gas entropies, heat capacities, and enthalpy corrections were calculated within the Rigid-Rotor Harmonic Oscillator approximation as implemented in the MultiWell package from the microscopic parameters (vibrational frequencies scaled by 0.9911 [14]). Hindered rotors, the potential energy surfaces of which were calculated at the level of theory M06-2x-D3/aug-cc-pVDZ, were accounted for. The recommended values are -457.4 kcal mol^{-1} and 117.8 cal mol^{-1} K^{-1} for the heat of formation and entropy, respectively, at room temperature.

4   Experimental Results

4.1 Ignition delay time measurements

The effect of a 10% of the H₂ concentration as DtFEC on the ignition delay time is visible in Fig. 2 for (a) $\phi = 0.5$, (b) 1.0, and (c) 2.0. As one can see, adding a small fraction of DtFEC leads to a significant increase in the activation energy of the mixture, corresponding to the slope of the data. This slope increase leads to a point where the two sets of data intersect, at a temperature that is dependent on the equivalence ratio: around 1450 K at $\phi = 0.5$, 1610 K at $\phi = 1.0$, and 1645 K at $\phi = 2.0$. For the longest delay time with the mixtures containing DtFEC, a factor of about 4 to 5 difference is observed with the neat mixture.

For the CH₄-based mixtures, Fig. 3, the activation energy of the data is not changed but a large effect is also visible. For all cases investigated, a noticeable decrease in the ignition delay time is observed when DtFEC is added to the mixture. This decrease in the delay is however dependent on the equivalence ratio: a factor of about 2.5-3.0 at $\phi = 0.5$, 2-2.5 at $\phi = 1.0$, and 1.5-2.0 at $\phi = 2.0$.
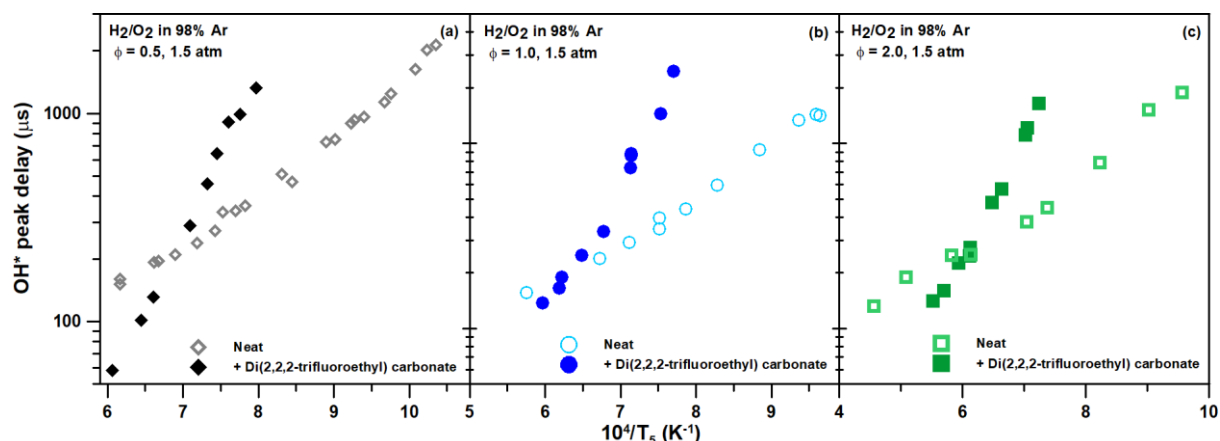

Figure 2: Comparison between the ignition delay time of H₂/O₂ mixtures in 98% Ar neat [8] and seeded with 10% of the H₂ concentration as DtFEC (balance Ar) ((a) $\phi = 0.5$, (b) $\phi = 1.0$, (c) $\phi = 2.0$).
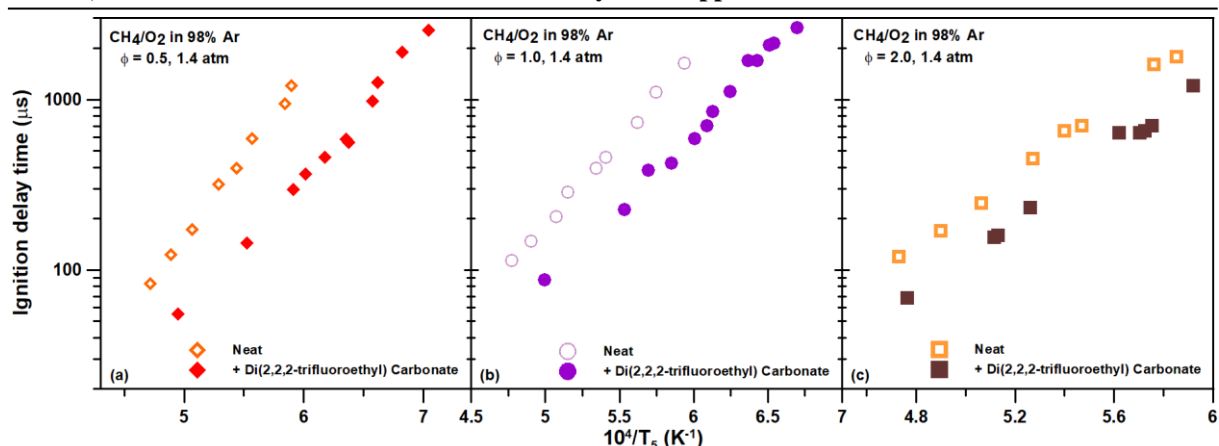
Figure 3: Comparison between the ignition delay time of CH_4/O_2 mixtures in 98% Ar neat [5] and seeded with 10% of the CH_4 concentration as DtFEC (balance Ar) ((a) $\phi = 0.5$, (b) $\phi = 1.0$, (c) $\phi = 2.0$).

3.2 Laminar flame speed measurements

The effect of DtFEC on the laminar flame speed of H_2-air mixtures and CH_4-air mixtures was studied in two ways. For each parent fuel, a concentration study was conducted by adding various concentrations of DtFEC (up to about 1% of the total mixture) to mixtures at a fixed ϕ, which was chosen to be near the respective peak flame speed for each fuel. For both fuels, an equivalence ratio study was also conducted for a fixed concentration of DtFEC of 0.5% over a full range of equivalence ratios.

The H_2 flame speed results are shown in Fig. 4. The results of the concentration study are shown in Fig. 4a, where the suppressing effect of DtFEC causes a drop of over 112 cm/s (or 40%) in flame speed for approximately 0.8% DtFEC. The effect is nonlinear, with increasing concentrations of DtFEC causing larger and larger decreases in flame speed. Included in Fig. 4a is a 2nd-order polynomial fit of the following equation: $LFS = 282.8 - 72.4 \times (\%DtFEC) - 87.6 \times (\%DtFEC)^2$, showing the nonlinear effect of DtFEC. The suppressing effect of DtFEC on H_2 is strongly dependent on ϕ, as shown in Fig. 4b. The baseline H_2-air data were reproduced from Krejci et al. [8]. The additive has a relatively small effect for lean mixtures, but the rich side suffers increasingly greater decreases in flame speed as ϕ increases. A maximum decrease of 121 cm/s (56%) was observed at ϕ=3.0. The decrease in flame speed on the lean side is somewhat masked by the steep slope of the curve. The lean DtFEC flames were approximately 7-11% slower than the neat flames. The addition of DtFEC also significantly lowers the upper flammability limit of H_2, as indicated by a mixture prepared at ϕ=3.5 which failed to ignite.
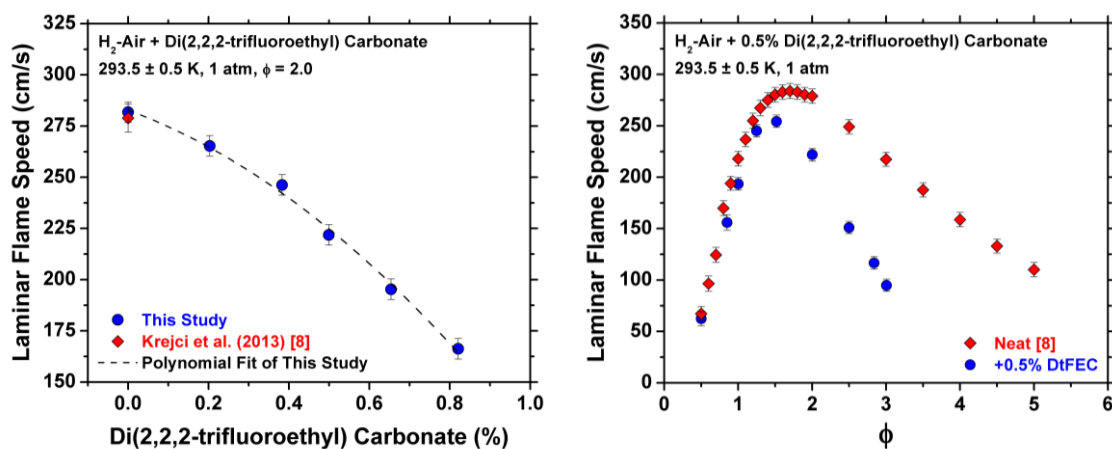

Figure 4: (a) Effect of various concentrations of DtFEC on H_2-air flame speed at ϕ=2.0. (b) Effect of 0.5% DtFEC on H_2-air flame speed across full range of equivalence ratio.

The CH$_4$ flame speed results are shown in Fig. 5. The concentration study in Fig. 5a shows that DtFEC has a linear effect on CH$_4$ flame speed, with 0.92% DtFEC causing a 42% drop in flame speed at ϕ=1.1. A linear fit is shown in Fig. 5a with the equation $LFS = 36.9 - 16.3 * (\%DtFEC)$. As shown in Fig. 5b, the suppressing effect of DtFEC varies with the equivalence ratio, with rich mixtures suffering greater decreases in flame speed than lean mixtures. Indeed, there was no measurable effect of DtFEC addition at ϕ=0.65, while the largest decrease (43%) was measured at ϕ=1.3. The baseline CH$_4$ data are reproduced from Turner et al. [9]. Although DtFEC causes a decrease in ignition delay time for CH$_4$ mixtures, the compound clearly behaves as a fire suppressant when considering laminar flame speed, indicating multiple competing effects on the kinetic pathways of CH$_4$ oxidation.
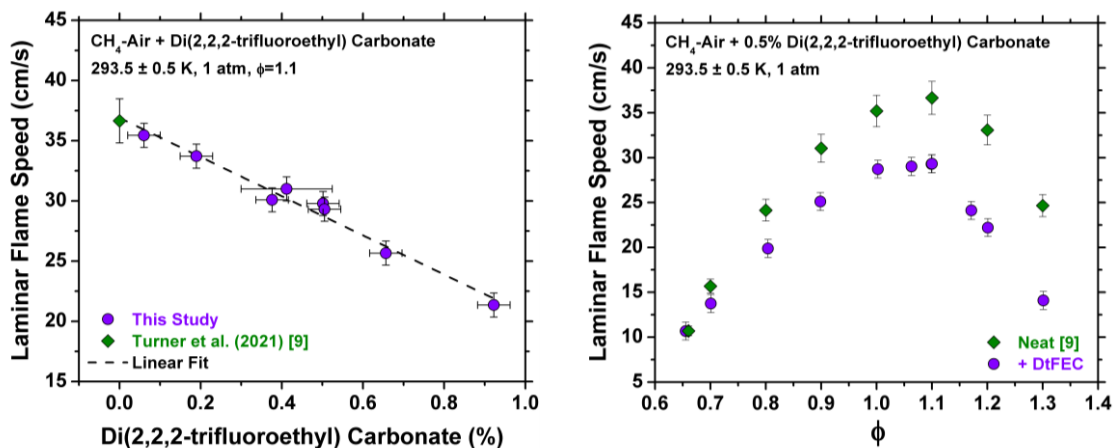

Figure 5: (a) Effect of various concentrations of DtFEC on CH$_4$-air flame speed at ϕ=1.1. (b) Effect of 0.5% DtFEC on CH$_4$-air flame speed across full range of equivalence ratio.

4   Conclusion

As an additive to CH$_4$ and H$_2$ mixtures, DtFEC causes various and sometimes unexpected effects on ignition and flame propagation. DtFEC caused a large increase in the activation energy of H$_2$, while the activation energy of CH$_4$ was unchanged. Even though DtFEC generally inhibited ignition of H$_2$, it also caused a decrease in H$_2$ ignition delay time at high enough temperatures. However, its effectiveness as a fire suppressant is clear in the large decrease in H$_2$ flame speed. For CH$_4$, DtFEC caused CH$_4$ ignition delay time to actually decrease for every tested temperature and equivalence ratio, even though DtFEC also caused decreased flame speed at every tested condition. The results included herein provide much-needed data for validating and improving chemical kinetics mechanisms for the target fire suppressant, of which currently there are none readily available to model these mixtures.

5   Acknowledgments

References

[1] Wang Q, Mao B, Stoliarov SI, and Sun J. (2019). A review of lithium ion battery failure mechanisms and fire prevention strategies. Prog. Energy Combust. Sci. 73: 95.

[2] Pham HQ, Lee H-Y, Hwang E-H, Kwon Y-G, and Song S-W. (2018). Non-flammable organic liquid electrolyte for high-safety and high-energy density Li-ion batteries. J. Power Sources. 404: 13.

[3] Shi P, Fang S, Luo D, Yang L, and Hirano S-i. (2017). A Safe Electrolyte Based on Propylene Carbonate and Non-Flammable Hydrofluoroether for High-Performance Lithium Ion Batteries. J. Electrochem. Soc. 164: A1991.

[4] Baird AR, Archibald EJ, Marr KC, and Ezekoye OA. (2020). Explosion hazards from lithium-ion battery vent gas. J. Power Sources. 446: 227257.

[5] Mathieu O, Goulier J, Gourmel F, Mannan MS, Chaumeix N, and Petersen EL. (2015). Experimental study of the effect of CF_3I addition on the ignition delay time and laminar flame speed of methane, ethylene, and propane. Proc. Comb. Inst. 35: 2731.

[6] Mathieu O, Keesee C, Gregoire C, and Petersen EL. (2015). Experimental and Chemical Kinetics Study of the Effects of Halon 1211 (CF_2BrCl) on the Laminar Flame Speed and Ignition of Light Hydrocarbons. The Journal of Physical Chemistry A. 119: 7611.

[7] Mathieu O, Sikes T, Kulatilaka WD, and Petersen EL. (2020). Ignition delay time and laminar flame speed measurements of mixtures containing diisopropyl-methylphosphonate (DIMP). Combust. Flame. 215: 66.

[8] Krejci MC, Mathieu O, Vissotski AJ, Ravi S, Sikes TG, Petersen EL, Kérmonès A, Metcalfe W, and Curran HJ. (2013). Laminar Flame Speed and Ignition Delay Time Data for the Kinetic Modeling of Hydrogen and Syngas Fuel Blends. J. Eng. Gas Turbines Power. 135: 021503.

[9] Turner MA, Paschal TT, Parajuli P, Kulatilaka WD, and Petersen EL. (2021). Application of high-speed, species-specific chemiluminescence imaging for laminar flame speed and Markstein length measurements in spherically expanding flames. Exp. Therm Fluid Sci. 129: 110477.

[10] Chen Z. (2011). On the extraction of laminar flame speed and Markstein length from outwardly propagating spherical flames. Combust. Flame. 158: 291.

[11] Sikes T, Mannan MS, and Petersen EL. (2018). An experimental study: laminar flame speed sensitivity from spherical flames in stoichiometric CH_4–air mixtures. Combust. Sci. Technol. 190: 1594.

[12] Zhao Y, and Truhlar DG. (2008). The M06 suite of density functionals for main group thermochemistry, thermochemical kinetics, noncovalent interactions, excited states, and transition elements: two new functionals and systematic testing of four M06-class functionals and 12 other functionals. Theor. Chem. Acc. 120: 215.

[13] Grimme S, Antony J, Ehrlich S, and Krieg H. (2010). A consistent and accurate ab initio parametrization of density functional dispersion correction (DFT-D) for the 94 elements H-Pu. J. Chem. Phys. 132: 154104.

[14] Kesharwani MK, Brauer B, and Martin JML. (2015). Frequency and Zero-Point Vibrational Energy Scale Factors for Double-Hybrid Density Functionals (and Other Selected Methods): Can Anharmonic Force Fields Be Avoided? The Journal of Physical Chemistry A. 119: 1701.